

Adeno-associated virus vector gene delivery elevates Factor I levels and down-regulates the complement alternative pathway *in vivo*.

Amina Ahmad¹, Mawj Mandwie¹, Anna K Dreismann², Christine M. Smyth¹, Helen Doyle³,
Talat H. Malik⁴, Matthew C. Pickering⁴, Peter J. Lachmann², Ian E. Alexander⁵ & Grant J.
Logan¹

¹ Gene Therapy Research Unit, Children's Medical Research Institute and Sydney Children's Hospitals Network, University of Sydney, Westmead, New South Wales, Australia.

² Department of Veterinary Medicine, University of Cambridge, Cambridge, UK

³ Pathology, Sydney Children's Hospitals Network, Westmead, New South Wales, Australia.

⁴ Centre for Inflammatory Disease, Imperial College London, UK.

^{1,5} Discipline of Child and Adolescent Health, University of Sydney, Westmead, Australia.

Correspondence: Grant J. Logan
Gene Therapy Research Unit
Children's Medical Research Institute
Locked Bag 23
Westmead NSW 2145
AUSTRALIA

Ph: +61-2-8865 2946

Fax: +61-2-8865 2801

Email: glogan@cmri.org.au

Short Title: AAV gene therapy to modulate the complement system *in vivo*

Keywords: adeno-associated virus, complement, factor I, alternative pathway, immune modulation

Abstract

The complement system is a key component of innate immunity but impaired regulation influences disease susceptibility, including age-related macular degeneration (AMD) and some kidney diseases. Whilst complete complement inhibition has been used successfully to treat acute kidney disease, key unresolved challenges include strategies to modulate rather than completely inhibit the system and to deliver therapy potentially over decades. Elevating concentrations of complement regulator factor I (CFI) restricts complement activation *in vitro* and this approach was extended in the current study to modulate complement activation *in vivo*. Sustained increases in CFI levels were achieved using an adeno-associated virus (AAV) vector to target the liver, inducing a 4- to 5-fold increase in circulating CFI levels. This led to decreased activity of the alternative pathway as demonstrated by a reduction in the rate of iC3b deposition and more rapid formation of C3 degradation products. In addition, vector application in a mouse model of systemic lupus erythematosus (NZBWF1), where tissue injury is in part complement dependent, resulted in reduced complement C3 and IgG renal deposition. Collectively, these data demonstrate that sustained elevation of CFI reduces complement activation *in vivo* providing proof-of-principle support for the therapeutic application of AAV gene delivery to modulate complement activation.

200 Words

Introduction

Complement is essential for maintaining tissue homeostasis through removal of apoptotic debris, processing of immune complexes and to provide protection against pathogens through opsonisation, direct cell lysis and promotion of adaptive immunity [1]. This critically important system provides a rapid response to pathogens, particularly early in life until adaptive immunity has been established, but tight regulation is necessary to prevent uncontrolled activation and inappropriate damage to host tissues. More than 30 cell-membrane and soluble proteins constitute three pathways, the activation of which is triggered by different stimuli. The classical pathway is initiated by antibody binding to antigen whilst the lectin pathway is initiated through lectins or ficolins binding to sugar residues on apoptotic/necrotic cells and microorganisms. Both pathways converge at a point where C3 is modified to form C3b initiating downstream production of the membrane attack complex (MAC) leading to proinflammatory responses and lytic destruction of complement-bound cells. The alternative pathway acts as an amplifier for the other pathways and is additionally activated when C3b is bound on a “protected” surface of which bacterial endotoxin (LPS) is an important example [2].

The alternative pathway (AP) is evolutionarily the oldest complement pathway and is centrally positioned to positively and negatively regulate the complement cascade [3]. The outcome of its activation is dependent on the net balance of two competing cycles (Figure 1). The AP is initiated when C3b binds a surface lacking complement regulatory proteins. This event recruits complement factor B (CFB) which, together with complement factor D, leads to the formation of a C3 convertase that converts more C3 to C3b. Left unchecked, this results in the rapid amplification of a pro-inflammatory response. In direct competition with this positive feedback cycle, the degradation cycle proteolytically removes C3b to prevent formation of C3 convertase. The degradation cycle is initiated when complement factor H (CFH) binds C3b and acts as a co-factor for complement factor I (CFI) to cleave C3b into “inactive C3b” (iC3b). This irreversibly removes C3b as a substrate for the feedback cycle and enables CFI, along with CR1 as a cofactor, to further cleave iC3b into C3c and C3dg. iC3b is itself an important generator of inflammation by its reaction with CR3 (CD11b,CD18) on neutrophils. Environments that favour activity of the

degradation cycle halt downstream MAC formation and subvert lytic destruction and pro-inflammatory responses.

Dysregulation of the complement system underlies a range of diseases acting as either the primary mediator of immunopathology or by amplifying stimuli triggered by genetic and/or environmental factors. This is evident from diseases that result from loss-of-function mutations in complement regulatory genes, for example Paroxysmal Nocturnal Haemoglobinuria (PNH) and atypical Haemolytic Uraemic Syndrome (aHUS) [4-6]. However, even subtle changes in the degree of complement activation driven by single nucleotide polymorphisms (SNPs) can influence disease susceptibility. It is now widely accepted that genetic variation in genes encoding complement activation and regulatory proteins, termed complotype [7], influences the threshold for complement activation [8-13]. A hyperactive (or 'at risk') complotype increases susceptibility to diseases such as AMD but is likely to have also provided an evolutionary advantage by reducing susceptibility to infection. In contrast, a hypoactive complotype confers AMD protection. Complement therapeutics to date have focused on complete inhibition of the system, notably C5 inhibition as an effective treatment for red cell lysis in PNH and for episodes of aHUS [14]. For diseases like AMD that develop over decades the intuitive approach is to reduce the complement activation threshold, essentially mimicking hypoactive complotypes that are associated with reduced AMD risk.

CFI is a serine protease and complement regulatory protein synthesised as a pro-enzyme predominantly in the liver where it is cleaved and secreted into plasma as an active enzyme [15]. *In vitro* serological studies have demonstrated that elevation of the levels of CFI is a powerful strategy to reduce AP activation in normal sera [16] as well as sera collected from individuals with hyperactive complotypes, known to place them at risk of AMD, aHUS and/or C3 glomerulopathy [17, 18]. A key finding was that AP activity of hyperactive complotypes could be reduced to within normal range using a modest 50% increase in CFI levels above endogenous concentrations (400g/mL) [18]. Based on these observations, sustained and persistent elevation of CFI levels *in vivo* offers a potential opportunity to reduce the negative effects of a hyperactive AP.

To deliver a therapeutic agent for long-term complement modulation *in vivo*, we sought to exploit adeno-associated virus (AAV) vector gene delivery. The system is proving clinically efficacious particularly for gene therapies in the eye, central nervous system and liver [19-22]. Importantly, AAV gene delivery to post-mitotic cells induces sustained transgene expression and therapeutic benefit, which has been observed in one haemophilia trial [19, 23] for more than ten years. A similar outcome in transgene expression with an F1-encoding vector might enable sustained suppression of AP activation and conversion of a genetically driven hyperactive complementotype into a therapeutically-driven hypoactive complementotype with consequent reduced incidence of disease.

The current report demonstrates that liver-directed AAV delivery of a CFI-encoding transgene cassette (AAV.CFI) elevated circulating CFI levels, which in turn decreased circulating AP activity. Using a well characterised murine model of systemic lupus erythematosus (SLE), where complement activation occurs within the kidney, AAV.CFI induced a significant reduction in renal co-deposition of complement and IgG. These proof-of-principle data support clinical translation of sustained elevation of CFI expression through AAV-mediated vector delivery to achieve therapeutic modulation of complement.

Results

AAV transgene delivery raises serum CFI levels *In vivo* and suppresses complement AP activity.

An AAV vector encoding murine CFI (AAV.CFI) under the transcriptional control of a liver-specific promoter (Figure 2A) was packaged and injected i.p. into C57BL/6 mice (5×10^{11} vg/mouse). Analysis of sera in time-course studies revealed a 4- to 5-fold increase in serum CFI levels within one week of AAV.CFI vector delivery, which were maintained for the duration of the 8-week experiments (Figure 2B). Western blot analysis confirmed elevated levels of a 50kDa protein in the AAV-CFI group, consistent with the molecular weight of the heavy chain of fully processed mouse CFI (Figure 2C). To assess AP inhibition, an iC3b deposition assay was performed using sera from mice treated at a range of vector doses (5×10^9 , 5×10^{10} or 5×10^{11} vg per mouse). AP inhibition in sera from AAV.CFI injected animals was evident by the dose-dependent reduction in iC3b deposition (Figure 3A). To

assess iC3b production by CFI, a C3b cleavage assay was performed which demonstrated increased production of C3dg in animals treated with the AAV.CFI vector (Figure 3B, Supplementary Figure 1). These data demonstrate that elevated levels of CFI *in vivo* favours activity of the AP degradation cycle and is consistent with published *in vitro* data [17, 18].

Elevated CFI levels are associated with reduced CFB levels but do not change C3, C5 and C7 levels.

Viral infections have been associated with acute phase responses that could alter complement protein concentrations [24, 25]. We therefore measured C3, C5 and C7 levels (Figure 4A-C and supplementary Figures 2 and 3) however there was no difference in circulating levels of these proteins between the AAV.CFI and AAV.GFP groups. In contrast, serum levels of CFB were elevated in AAV.CFI treated animals (Figure 4D, Supplementary Figure 4). The higher levels of CFB were not attributed to enhanced transcriptional activity from the CFB gene in the liver, which is the predominant source of the protein [26], as mRNA levels remained unchanged in control and test animals (Figure 4E).

AAV.CFI reduces renal deposition of C3 and IgG in AAV.CFI-treated lupus-prone mice.

We next sought to test the ability of AAV.CFI to modulate tissue complement deposition in a disease model. The lupus-prone NZBWF1 mouse model was utilised as renal complement deposition is a feature of the phenotype [27]. As expected, mean serum CFI levels at two months post-injection were increased in the AAV.CFI treated group, although with a broad spread of levels (Figure 5A). However, by end-of-life CFI levels were indistinguishable between the groups. Many AAV.CFI treated mice showed reductions in CFI levels whilst some of the AAV.GFP treated mice exhibited CFI levels higher than AAV.CFI treated mice (Figure 5A, Supplementary figure 5). Vector copy number analysis at end-of-life showed a broad spread of values within each group but no statistical difference between each group (Figure 5B). This finding might be due to loss of provirus in some animals over time. There was a strong correlation between AAV.CFI vector copy number and CFI mRNA levels (Figure 5C, Pearson $r=0.96$) at end-of-life but a poor correlation between AAV.CFI vector copy number and serum CFI levels (Figure 5D). Antibodies to CFI that might account for variable CFI protein levels were not detected (data not shown). In contrast, antibodies to

the AAV8 capsid were detected (as expected) two months after vector injection, which then decreased over time (Supplementary Figure 5). This data collectively indicate dysregulation of CFI expression from the endogenous locus and/or vector transgene with age in NZBWF1 mice, consistent with changes in gene [24] and transgene expression with increasing inflammation [28].

It was hypothesised that elevated levels of CFI in AAV.CFI treated mice, through control of the C3b amplification loop, would reduce glomerular C3 and associated IgG in the lupus-prone mice. Immunofluorescence analysis of kidney sections showed a significant reduction in glomerular IgG (Figure 6A-B) and C3 deposition (Figure 6C-D) in the glomeruli of AAV.CFI treated animals. However, there were no differences in either renal function or glomerular histology (Figure 7). and AAV.CFI treatment did not alter survival, serum immune complexes, anti-ssDNA antibodies, spleen pathology or glomerular neutrophil infiltration (Supplementary Figure 6). Collectively, these data indicate that while treatment with AAV.CFI exerted biological effects that led to reduced renal IgG and C3 deposition, which are classic hallmarks of SLE, these were insufficient to confer renal protection or improve disease outcome in the NZBWF1 mouse model.

Discussion

The current study demonstrates that the AP can be modulated *in vivo* by raising serum levels of CFI to inhibit complement activation. This was evident by the change in levels of C3 breakdown products in wild type mice as well as inhibition of renal C3/IgG deposition in lupus-prone mice. The raised levels of serum CFB in AAV.CFI treated C57BL/6 mice is also interpreted as evidence for decreased consumption of CFB in the feedback cycle through increased activity of the degradation cycle. These *in vivo* findings validate earlier *in vitro* studies [17, 18] demonstrating the potential for AP modulation by increased CFI levels to reduce disease susceptibility in individuals with hyperactive complementotypes.

Importantly, the current study also shows that AAV-mediated gene delivery is a feasible approach to achieve AP modulation in the SLE NZBWF1 mouse model. This model was selected because it was hypothesised that AAV.CFI may reduce renal deposition of C3, which in this model is due to classical pathway activation by immune complexes.

Moreover, other studies have shown that reduction of complement activation, through either down-regulation of factor B (Grossman et al. 2016) or administration of complement inhibitors [29, 30], reduced phenotypic endpoints in this model. We demonstrated that AAV.CFI reduced IgG/C3 deposition in the kidney, however the vector was unable to arrest natural disease progression or extend animal lifespan. This is not surprising since complement is only one of the many effector mechanisms of tissue injury in this model [31]. In the MRL/lpr lupus model, complement C3 was not required for the development of immune-complex nephritis [32]. The precise mechanism by which higher CFI serum concentrations decreased renal IgG/C3 levels remains to be determined but could be due to interference in complement deposition through a more active degradation cycle and/or improved removal of tissue immune complexes. Irrespectively, these collective findings support the hypothesis that elevated CFI levels exert biological effects that may be exploited for therapeutic gain.

Normalisation of AP regulation via a single vector infusion as opposed to recurrent systemic infusions of recombinant CFI is an appealing clinical proposition. The recent successes using liver-targeted AAV vectors to treat haemophilia A and B patients demonstrates AAV vector technologies are well-positioned for the task [19, 22]. This goal has become even more feasible with the recent identification of hepatotropic capsids inducing higher vector transfer efficiencies compared to those used in early clinical trials [33-35]. Additionally, AP regulation through elevated CFI levels avoids issues with immunogenicity as CFI is normally expressed in the liver and the immunobiology of this organ enforces tolerance to the transgene product [36]. Furthermore, CFI is expressed at relatively low levels (40 μ g) making the predicted need for a 50% increase in systemic levels for AP regulation [18] a more feasible target when compared to over-expression of CFH, a regulatory protein that also dampens activity of the feedback cycle when levels are elevated but which is expressed at 200 μ g/mL in serum [37].

The results of the current study demonstrate the potential for liver-targeted AAV to prevent a number of diseases in individuals with an 'at-risk' hyperactive complotype [1, 7]. Dry AMD is a prime target for AP modulation given its association with the hyperactive complotype [6, 8, 11-13]. However, it has been reported that the intact Bruch's membrane

in the eye is impervious to CFI diffusion from the circulation and that ocular AP regulation requires local secretion of regulatory proteins [13]. If this is the case, intervention using AAV.CFI would require sub-retinal rather than liver delivery of the vector and such a trial is already underway (NCT03846193,[38]). In theory, the earlier the intervention the higher the likelihood of preventing AMD but further investigation is required to delineate whether the cellular source of CFI in the eye is important for AP regulation. At least from the perspective of vector production, AAV ocular gene delivery is a more appealing route given the need for lower amounts of vector compared to liver-targeted systemic delivery.

The possibility for deleterious effects in raising systemic CFI levels has also been considered. In the rare setting of uncontrolled C3 activation due to complete CFH deficiency, abnormal accumulation of C3 occurs within glomeruli resulting in C3 glomerulopathy. In mouse models, the intra-glomerular localisation of the abnormal C3 in complete CFH deficiency is influenced by CFI [39]. In the absence of CFI, the abnormal glomerular C3 is not cleaved beyond C3b and localises within the mesangium. In contrast, in the presence of CFI, C3 is accumulated along the capillary walls and results in renal disease. It is therefore possible that in situations in which factor H function is severely impaired, increasing CFI levels may be deleterious. Further advancement of the AAV technology would benefit from the validation of this approach in pre-clinical models of complement-mediated disease. The major strength of this approach would be to treat diseases, such as AMD, which are chronic and would be predicted to require complement modulation over the long term to achieve benefit. However, an AAV-mediated approach might be applicable in other settings and could be applied to express the many complement inhibitors and modulators in development [1]. In conclusion, this preclinical study supports translation of AAV gene delivery as a viable approach to complement modulation *in vivo*.

Author Contributions

A.A., M.M., A.K.D., M.C.P., P.J.L., I.E.A. & G.J.L. designed the experiments. A.A., M.M., A.K.D., C.M.S., H.D., T.H.M., M.C.P., P.J.L., I.E.A. & G.J.L. generated reagents, algorithms, protocols, performed experiments, analysed and interpreted the data. M.C.P., A.A., M.M.,

I.E.A. & G.J.L. wrote the manuscript and generated the figures. All authors reviewed, edited and commented on the manuscript.

Disclosure/Conflict of Interest

Some authors have an affiliation with Gyroscope Therapeutics, a biotechnology company that seeks to commercialize AAV-mediated complement modulation for ocular therapies. Specifically, PJJ is a co-founder of the company, MCP is on the scientific advisory board, AKD is an employee and GJL is a past-employee.

Material and Methods

Mouse studies

All animal care and experimental procedures were evaluated and approved by the CMRI/CHW Animal Care and Ethics Committee. All C57BL/6 and NZBWF1 mice used in this study were bred in-house from breeding pairs obtained from The Jackson Laboratories (Bar Harbor, ME). Mice were housed in standard boxes and received normal food and water *ad libitum* for the duration of the experiments. Animals were injected via the intraperitoneal route at 6-12 weeks of age with 100 μ L of the indicated vector quantities after dilution in saline. Animals were culled when displaying signs of illness and pain, such as shallow breathing, swollen cheeks, hunched posture or weight loss.

Serum collection

Blood was collected using either the tail vein nicking or cardiac puncture (terminal) method into uncoated collection tubes (Becton Dickinson). For cardiac puncture, mice were anaesthetised by isoflurane inhalation and cardiac puncture performed with a 25-gauge needle. Blood was left to clot for 30-40 minutes at room temperature, then centrifuged at 3,000 $\times g$ for 5 minutes. The serum was then taken and centrifuged again at 20,000 $\times g$ for 5 minutes to eliminate any residual red blood cells. Serum was aliquoted and stored at -80°C.

Urine collection

Urine was collected for analysis of protein and creatinine levels. Mice were placed in metabolic cages lined with Whatman paper for 24 hours. The filter papers with urine were

then collected, dried overnight and stored at 4°C. When required for analysis, 10 circular holes (approximately 3 mm in diameter) were punched into urine-stained areas on the filter paper and dissolved in 300 µL of water for approximately 2 hours at room temperature. The tubes were centrifuged for 1-2 minutes at 4,000 × g and the supernatant collected for biochemical analyses.

Biochemical Analysis

Creatinine and protein analysis was performed by The Department of Pathology, Westmead Children's Hospital. Creatinine analysis in the serum was determined by an enzymatic assay kit (Mouse Creatinine Assay Kit no. 80350, Crystal Chem).

Plasmid and vector production

The AAV.GFP has been previously reported [40]. It contains AAV2 ITR sequences flanking an expression cassette consisting of heterologous (one copy of the *SERPINA1* (hAAT) promoter, two copies of the *APOE* enhancer element upstream), a GFP-encoding cDNA, variant (mut6) of the woodchuck hepatitis virus post-transcriptional regulatory element (WPRE) and bovine polyadenylation signal. The AAV-FI construct was produced using standard molecular biological techniques by replacing the GFP cDNA with one encoding murine FI.

AAV vectors packaged into capsid 8 were made using triple-transfection of HEK-293 cells (obtained from the American Type Culture Collection) as previously described [41]. Briefly, HEK-293 cells were cultured in plastic culture dishes with complete medium (DMEM containing 10% FBS) were passaged using trypsin. Cells transfected with packaging constructs were subjected to four freeze/thaw cycles in a dry ice/100% ethanol bath, centrifuged at 3000 x g for 15 minutes and the supernatant was treated with benzonase (Sigma Aldrich) at 50 units/mL at 37°C for 30 minutes. Vector was purified using CsCl purification. Final viral titre was assigned by qPCR [42]. Purified vector was aliquoted and stored at -80°C.

Quantitation of liver vector copy number and mRNA encoding FI and CFB.

Liver was snap frozen in liquid nitrogen and stored at -80°C for later assay. DNA was extracted using proteinase K digestion and phenol:chloroform extraction as previously

described [42]. RNA was extracted using the Trizol[®] plus RNA purification kit (Ambion) following the manufacturer's instructions. DNA and RNA concentrations were determined by spectrophotometry using a Nanodrop 1000 (Thermo Fisher Scientific, Wilmington, USA). Total RNA was reversed transcribed into cDNA using the SuperScript[®] III Reverse Transcriptase kit (Invitrogen) according to the manufacturer's instructions. Quantitative PCR (qPCR) reactions were performed using a RotorGene 6000 (Corbett Life Science, Mortlake, Australia). Vector provirus copy number was calculated from genomic DNA using primers specific to the WPRE region on the vector and were normalised to GAPDH levels quantified using SYBR Green (Takara). FI and CFB mRNA levels were quantified by qPCR on cDNA samples using target specific primers and signals were normalised against β -actin levels also determined by qPCR. Primer sequences are detailed in Supplementary Table 2.

Western blot for complement proteins.

Western blot was performed on serum samples after probing blots using the following primary antibodies: anti-FI polyclonal antibody (, Absea Biotechnology Ltd.), goat anti-mouse C3 polyclonal (Cappel #0855444), goat anti-C5 polyclonal (Dako P0449), rabbit anti-human CFB polyclonal (Abcam ab192577) or Rabbit anti-C7 polyclonal (Abcam ab192346). After washing to remove the primary antibodies, blots were further probed using either of the following HRP-conjugated secondary antibodies: goat anti-rabbit IgG (Santa Cruz sc-2004), rabbit anti-goat IgG (Dako P0449), anti-mouse IgG (Dako P0447) or goat anti-rabbit IgG (Santa Cruz sc-2004). Signals were detected using Supersignal[™] West femto chemiluminescent substrate (Thermofisher) and visualised on the Fujifilm LAS4000 (Berthold). Blots were stripped using a solution containing glycine (25mM), SDS (1.5% SDS w/v) dissolved in distilled water washed and probed using antibodies to vinculin (Sigma V9131) and re-imaged. Western Blot imaging analysis was performed using Image J (Fiji) and signals were normalised to vinculin.

CFI quantitation dot blot

Serum CFI levels were quantitated using ELISA (CSB-EL005279MO) or dot blot as indicated. A dot blot was performed on serum samples to detect murine Factor I protein levels.

Double dilutions of serum samples were made from 1 in 80 to 1 in 640 in sample buffer (62.5mM Tris-Cl pH 6.8, 0.05% SDS, 0.36M β -mercaptoethanol). Purified Factor I double dilutions in sample buffer from 2.5ng/ μ L to 0.3ng/ μ L were also included. Samples were heated at 70⁰C for 10 minutes and 100 μ L was loaded directly into each well of the dot blot apparatus. Suction was used to allow the liquid to pass through the wells and onto the nitrocellulose membrane (Bio-rad). Wells were rinsed with 200 μ L of PBST [PBS/0.05% Tween-20 (Sigma-Aldrich)], allowing suction to pass through the membrane until wells were dry. The apparatus was then disassembled, and membranes were washed with PBST and blocked with 20 mL of 5% milk/PBST for 1 hour while gently rocking on the shaker at room temperature. After blocking, the solution was removed, and membranes were incubated with rabbit anti-murine CFI antibody (Absea Biotechnology Ltd.) followed by secondary antibody incubation with goat anti-rabbit (Santa Cruz sc-2004) for 1 hour at 4⁰C, washing and imaging as previously mentioned for western blot.

iC3b Deposition assay

Maxisorb Nunc Plates were coated overnight with 1 μ g/well of lipopolysaccharide (Sigma) from *Escherichia coli* O26:B6 in coating buffer (15mM Na₂CO₃, 35mM NaHCO₃ pH 9.6) at 4⁰C. Plates were then washed 3 times with 200 μ L of TBST (10mM Tris-HCl, 140mM NaCl, 0.05% Tween-20 pH 7.4) and blocked with 100 μ L of 1%BSA in TBS-T at room temperature for 2 hours. After washing, plates were incubated with serial dilutions of serum in alternative pathway buffer (1xVBS, 10mM EGTA, 2mM MgCl₂) for 1 hour at 37⁰C. Plates were washed 4 times with TBS-T and incubated for 1 hour with polyclonal rabbit α -human C3c complement (Dako A0062), used 1:5000 in TBS-T. After washing 4 times with TBS-T, wells were incubated for 1 hour with alkaline phosphatase conjugated goat anti-rabbit IgG (Sigma Aldrich A3812) at a 1:5000 dilution in TBS-T. The plates were then washed 4 times with TBS-T and 100 μ L of prepared Fast p-Nitrophenyl Phosphate Tablets (Sigma N1891) was added to develop the assay which was stopped by addition of 3M NaOH and read at 405nm.

AAV8 IgG ELISA

Maxisorb Nunc 96-well plates were coated overnight with 2.5 x 10¹⁰ vg/mL of AAV8 in 0.1M NaHCO₃ at 4⁰C. Plates were then washed 3 times with 200 μ L of washing buffer (PBS

with 0.05% Tween-20, PBST) and blocked with 100 μ L of PBST supplemented with 5% Skim (PBST+5% skim milk powder, PBST-skim) at room temperature for 2 hours. After washing, plates were incubated for two hours at room temperature with 50 μ L of sera diluted in PBST-skim in 2-fold serial dilutions starting at a 1:50 dilution. Plates were washed 3 times and incubated for 1 hour with goat anti-mouse IgG (Biorad Cat# 172-1011, diluted at 1:2000 in PBST-skim). After washing 4 times, 100 μ L of TMB (Sigma) was added to the wells and incubated for 30 minutes in the dark to develop the assay which was stopped by addition of 100 μ L of 1M H₂SO₄ and read at 450nm. The ratio of the mean of the OD values obtained with and without vector were calculated and endpoint titres were identified as the reciprocal of the last serum dilution that produced a ratio >2.0.

C3 ELISA

Maxisorb Nunc Plates were coated overnight with 1 μ g/well of polyclonal rabbit anti-human C3c complement (Dako A0062) in 0.1M NaHCO₃ at 4°C. Plates were then washed 3 times with 200 μ L of washing buffer (PBS with 0.2% Tween-20) and blocked with 100 μ L of 2% BSA in wash buffer at room temperature for 2 hours. After washing, plates were incubated with serial dilutions of C3 standard (Comptech #A113) and samples at 1 in 24000 dilution in blocking buffer for 1 hour. Plates were washed 5 times and incubated for 1 hour with goat anti-mouse C3 HRP (MP Biomedical Cat# 55557), used 1:25000 in wash buffer. After washing 5 times, 100 μ L of TMB (Sigma) was added to the wells and incubated for 15 minutes in the dark to develop the assay which was stopped by addition of 100 μ L of 1M H₂SO₄ and read at 450nm.

Serum immune complex ELISA

Serum immune complexes were assayed as described previously [43]. Briefly, Maxisorb Nunc Plates (ThermoFisher) were coated overnight with 2 μ g/mL of bovine conglutinin in coating buffer [0.0125 M sodium borate, 0.0125 M boric acid, 0.01 M CaCl₂ (pH 8.2)] at 4°C. Plates were then washed 3 times with 200 μ L of wash buffer [0.0125 M sodium borate, 0.0125 M boric acid, 0.01 M CaCl₂, 0.05% (v/v) Tween-20 (pH 8.2)] and blocked with 200 μ L of 2% (w/v) BSA in coating buffer at room temperature for 2 hours. After washing, plates were incubated with serum diluted 1 in 130 in wash buffer for 1 hour at room temperature. Plates were washed 4 times and incubated for 1 hour at room

temperature with goat anti-mouse IgG-AP (Sigma A3562) diluted 1:1,000 in wash buffer. The plates were then washed 4 times and 100 μ L of prepared Fast p-Nitrophenyl Phosphate Tablets (Sigma) was added to develop the assay which was stopped by addition of 3M NaOH and the absorbance of each well was measured at a wavelength of 405nm on the VersaMax microplate reader.

Anti-ssDNA ELISA

Anti-ssDNA antibodies were assayed as described previously [44]. Briefly, Maxisorb Nunc Plates (Thermofisher) were coated overnight with 10 μ g/mL of ssDNA (Sigma D8899) in coating buffer (1x PBS) at 4°C. Plates were then washed 3 times with 200 μ L of wash buffer [1x PBS, 0.05% (v/v) Tween-20] and blocked with 200 μ L of 3% (w/v) BSA in wash buffer at room temperature for 2 hours. After washing, plates were incubated with serum diluted 1 in 100 and serial dilutions of anti-ssDNA antibody (Abcam ab27156) from 0.2 ng/mL in wash buffer for 1 hour at room temperature. Plates were washed 4 times and incubated for 1 hour at room temperature with goat anti-mouse IgG-AP (Sigma A3562) diluted 1:1,000 in wash buffer. The plates were then washed 4 times and 100 μ L of prepared Fast p-Nitrophenyl Phosphate Tablets (Sigma N1891) was added to develop the assay which was stopped by addition of 3M NaOH and the absorbance of each well was measured at a wavelength of 405nm on the VersaMax microplate reader.

C3 and IgG deposition staining

Fixed mouse kidney tissue in frozen OCT blocks were cut into 5 μ M sections using the Leica CM1900 cryostat. Sections were re-hydrated with PBS for 10 minutes then placed in a coplin jar with cold methanol (-20°C) on ice for 15 minutes to permeabilize the sections. Slides were washed PBS, then dried and sealed with PAPEN (Sigma-Aldrich). Slides were blocked with 250 μ L of 20% (v/v) goat serum (Sigma) per slide for 3 hours. Blocking buffer was removed and the slides were incubated with anti-mouse IgG (Sigma-Aldrich F0257) or anti-mouse C3 (MP Biomedical 0855500) conjugated to FITC in blocking buffer at 4°C in a moist chamber for 1 hour in the dark. Slides were washed 3 \times 5 minutes with PBS and to the second wash, 10 μ L DAPI (Thermofisher) was added. Slides were dried and covered with 2 drops of Immunomount and a coverslip then imaged using Zeiss microscope under

DAPI and Texas Red fluorescence. Images and mean fluorescence intensities were taken using the ZEN software.

Neutrophil staining

Fixed mouse tissue in frozen OCT blocks were cut into 6µm sections using the Leica CM1900 cryostat. Sections were allowed to adhere to the slides and then fixed in acetone for 10 minutes. Slides were air dried for 5 minutes, sealed with PAPEN (Sigma-Aldrich) and then blocked with 10% Rat serum (Sigma) in 5%BSA/1xPBS for 60 minutes. Blocking buffer was removed and the slides were incubated with Alexa Fluor® 594 anti-mouse Ly-6G Antibody (BioLegend Cat#127636, 1/200 diluted in 1% BSA/1xPBS) overnight at 4°C covered in foil in a humid chamber. Slides were washed 2 × 5 minutes with PBS in the dark and 10 µL DAPI (Thermofisher) was added to the third wash. Slides were washed, dried and covered with 2 drops of Immunomount, coverslipped and imaged using Zeiss microscope. Images and quantification were performed using the ZEN software.

Assessment of H&E stained kidney and spleen

Paraffin embedded tissue was prepared as 5 µM sections using the Leica RM2235 microtome and sections were stained using standard staining protocols. Brightfield/light microscope imaging of sections was performed on an Axio Imager A1 using a Spot Insight Colour camera for taking images using Spot Version 4.0 software. All sections were assessed in a blinded fashion and graded. Kidney sections were scored based on the Jablonski scale of injury [45]. Spleen pathology was graded based on the percentage of red pulp replaced by extramedullary haematopoiesis and the presence or absence of germinal centres within the white pulp of the spleen.

Statistical Analysis

Data were analysed using GraphPad Prism Ver 8.4.0. Statistical analysis was performed using non-parametric two-tailed Mann Whitney Test or the Chi Square Test for certain pathology analysis to assess for significance. Survival curve was analysed using the Kaplan Meier method. p values of <0.05 were considered significant.

Acknowledgements

GJL received funding support from the Rebecca L Cooper Foundation (PG2019449). We are grateful to Szun Tay for technical expertise and Virginia James (Westmead Institute for Medical Research) for embedding and staining tissue sections.

References

1. Morgan, B.P. and L.C. Harris, *Complement, a target for therapy in inflammatory and degenerative diseases*. Nature Reviews Drug Discovery, 2015. **14**(12).
2. Lachmann, P.J., *Looking back on the alternative complement pathway*. Immunobiology, 2018. **223**(8-9): p. 519-523.
3. Lachmann, P.J., *The amplification loop of the complement pathways*, in *Advances in Immunology*. 2009. p. 115-149.
4. Botto, M., M. Kirschfink, P. Macor, M.C. Pickering, R. Würzner, and F. Tedesco, *Complement in human diseases: Lessons from complement deficiencies*. Mol Immunol, 2009. **46**(14): p. 2774-83.
5. Barbour, T.D., M.C. Pickering, and H.T. Cook, *Recent insights into C3 glomerulopathy*. Nephrol Dial Transplant, 2013. **28**(7): p. 1685-93.
6. Medjeral-Thomas, N. and M.C. Pickering, *The complement factor H-related proteins*. Immunol Rev, 2016. **274**(1): p. 191-201.
7. Harris, C.L., M. Heurich, S.R.D. Cordoba, and B.P. Morgan, *The complotype: dictating risk for inflammation and infection*. Trends in Immunology, 2012. **33**(10): p. 513-521.
8. Hageman, G.S., D.H. Anderson, L.V. Johnson, L.S. Hancox, A.J. Taiber, L.I. Hardisty, J.L. Hageman, H.A. Stockman, J.D. Borchardt, K.M. Gehrs, et al., *A common haplotype in the complement regulatory gene factor H (HF1/CFH) predisposes individuals to age-related macular degeneration*. Proc Natl Acad Sci U S A, 2005. **102**(20): p. 7227-32.
9. Pickering, M.C., E.G. De Jorge, R. Martinez-Barricarte, S. Recalde, A. Garcia-Layana, K.L. Rose, J. Moss, M.J. Walport, H.T. Cook, S.R. De Córdoba, et al., *Spontaneous hemolytic uremic syndrome triggered by complement factor H lacking surface recognition domains*. J Exp Med, 2007. **204**(6): p. 1249-56.
10. Heurich, M., R. Martínez-Barricarte, N.J. Francis, D.L. Roberts, S. Rodríguez De Córdoba, B.P. Morgan, and C.L. Harris, *Common polymorphisms in C3, factor B, and factor H collaborate to determine systemic complement activity and disease risk*. Proc Natl Acad Sci U S A, 2011. **108**(21): p. 8761-6.

11. Gold, B., J.E. Merriam, J. Zernant, L.S. Hancox, A.J. Taiber, K. Gehrs, K. Cramer, J. Neel, J. Bergeron, G.R. Barile, et al., *Variation in factor B (BF) and complement component 2 (C2) genes is associated with age-related macular degeneration*. Nat Genet, 2006. **38**(4): p. 458-62.
12. Kavanagh, D., Y. Yu, E.C. Schramm, M. Triebwasser, E.K. Wagner, S. Raychaudhuri, M.J. Daly, J.P. Atkinson, and J.M. Seddon, *Rare genetic variants in the CFI gene are associated with advanced age-related macular degeneration and commonly result in reduced serum factor I levels*. Hum Mol Genet, 2015. **24**(13): p. 3861-70.
13. Hallam, T.M., K.J. Marchbank, C.L. Harris, C. Osmond, V.G. Shuttleworth, H. Griffiths, A.J. Cree, D. Kavanagh, and A.J. Lotery, *Rare Genetic Variants in Complement Factor I Lead to Low FI Plasma Levels Resulting in Increased Risk of Age-Related Macular Degeneration*. Invest Ophthalmol Vis Sci, 2020. **61**(6): p. 18.
14. Mastellos, D.C., D. Ricklin, and J.D. Lambris, *Clinical promise of next-generation complement therapeutics*. Nat Rev Drug Discov, 2019. **18**(9): p. 707-729.
15. Lachmann, P.J., *The Story of Complement Factor I*. Immunobiology, 2019.
16. Lachmann, P.J. and L. Halbwachs, *The influence of C3b inactivator (KAF) concentration on the ability of serum to support complement activation*. Clinical and Experimental Immunology, 1975. **21**(1): p. 109-114.
17. Lay, E., S. Nutland, J.E. Smith, I. Hiles, R.a.G. Smith, D.J. Seilly, A. Buchberger, W. Schwaeble, and P.J. Lachmann, *Complotype affects the extent of down-regulation by Factor I of the C3b feedback cycle in vitro: In-vitro effects of complotype*. Clinical & Experimental Immunology, 2015. **181**(2): p. 314-322.
18. Lachmann, P.J., E. Lay, D.J. Seilly, A. Buchberger, W. Schwaeble, and J. Khadake, *Further studies of the down-regulation by Factor I of the C3b feedback cycle using endotoxin as a soluble activator and red cells as a source of CR1 on sera of different complotype*. Clinical and Experimental Immunology, 2016. **183**(1): p. 150-156.
19. Nathwani, A.C., E.G. Tuddenham, S. Rangarajan, C. Rosales, J. McIntosh, D.C. Linch, P. Chowdary, A. Riddell, A.J. Pie, C. Harrington, et al., *Adenovirus-associated virus vector-mediated gene transfer in hemophilia B*. N Engl J Med, 2011. **365**(25): p. 2357-65.

20. Russell, S., J. Bennett, J.A. Wellman, D.C. Chung, Z.F. Yu, A. Tillman, J. Wittes, J. Pappas, O. Elci, S. Mccague, et al., *Efficacy and safety of voretigene neparvovec (AAV2-hRPE65v2) in patients with RPE65-mediated inherited retinal dystrophy: a randomised, controlled, open-label, phase 3 trial*. *Lancet*, 2017. **390**(10097): p. 849-860.
21. Mendell, J.R., S. Al-Zaidy, R. Shell, W.D. Arnold, L.R. Rodino-Klapac, T.W. Prior, L. Lowes, L. Alfano, K. Berry, K. Church, et al., *Single-Dose Gene-Replacement Therapy for Spinal Muscular Atrophy*. *N Engl J Med*, 2017. **377**(18): p. 1713-1722.
22. George, L.A., M.V. Ragni, B.J. Samelson-Jones, A. Cuker, A.R. Runoski, G. Cole, F. Wright, Y. Chen, D.J. Hui, K. Wachtel, et al., *Spk-8011: Preliminary Results from a Phase 1/2 Dose Escalation Trial of an Investigational AAV-Mediated Gene Therapy for Hemophilia a*. *Blood*, 2017. **130**(Suppl 1): p. 604.
23. Nathwani, A.C., U.M. Reiss, E.G.D. Tuddenham, C. Rosales, P. Chowdary, J. McIntosh, M. Della Peruta, E. Lheriteau, N. Patel, D. Raj, et al., *Long-Term Safety and Efficacy of Factor IX Gene Therapy in Hemophilia B*. *The New England Journal of Medicine*, 2014. **371**(21): p. 1994-2004.
24. Jain, S., V. Gautam, and S. Naseem, *Acute-phase proteins: As diagnostic tool*. *J Pharm Bioallied Sci*, 2011. **3**(1): p. 118-27.
25. Perez, L., *Acute phase protein response to viral infection and vaccination*. *Arch Biochem Biophys*, 2019. **671**: p. 196-202.
26. Koskimies, S., M.L. Lokki, and K. Höckerstedt, *Changes in plasma complement C4 and factor B allotypes after liver transplantation*. *Complement Inflamm*, 1991. **8**(5-6): p. 257-60.
27. Richard, M.L. and G. Gilkeson, *Mouse models of lupus: what they tell us and what they don't*. *Lupus science & medicine*, 2018. **5**(1): p. e000199-e000199.
28. Breous, E., S. Somanathan, P. Bell, and J.M. Wilson, *Inflammation promotes the loss of adeno-associated virus-mediated transgene expression in mouse liver*. *Gastroenterology*, 2011. **141**(1): p. 348-57, 357.e1-3.

29. Grossman, T.R., L.A. Hettrick, R.B. Johnson, G. Hung, R. Peralta, A. Watt, S.P. Henry, P. Adamson, B.P. Monia, and M.L. Mccaleb, *Inhibition of the alternative complement pathway by antisense oligonucleotides targeting complement factor B improves lupus nephritis in mice*. Immunobiology, 2016. **221**(6): p. 701-708.
30. Sekine, H., P. Ruiz, G.S. Gilkeson, and S. Tomlinson, *The dual role of complement in the progression of renal disease in NZB/W F(1) mice and alternative pathway inhibition*. Mol Immunol, 2011. **49**(1-2): p. 317-23.
31. Lorenz, G. and H.J. Anders, *Neutrophils, Dendritic Cells, Toll-Like Receptors, and Interferon- α in Lupus Nephritis*. Semin Nephrol, 2015. **35**(5): p. 410-26.
32. Sekine, H., C.M. Reilly, I.D. Molano, G. Garnier, A. Circolo, P. Ruiz, V.M. Holers, S.A. Boackle, and G.S. Gilkeson, *Complement component C3 is not required for full expression of immune complex glomerulonephritis in MRL/lpr mice*. J Immunol, 2001. **166**(10): p. 6444-51.
33. Lisowski, L., A.P. Dane, K. Chu, Y. Zhang, S.C. Cunningham, E.M. Wilson, S. Nygaard, M. Grompe, I.E. Alexander, and M.A. Kay, *Selection and evaluation of clinically relevant AAV variants in a xenograft liver model*. Nature, 2014. **506**(7488): p. 382-386.
34. Paulk, N.K., K. Pekrun, E. Zhu, S. Nygaard, B. Li, J. Xu, K. Chu, C. Leborgne, A.P. Dane, A. Haft, et al., *Bioengineered AAV Capsids with Combined High Human Liver Transduction In Vivo and Unique Humoral Seroreactivity*. Molecular Therapy, 2018. **26**(1): p. 289-303.
35. Cabanes-Creus, M., A. Westhaus, R.G. Navarro, G. Baltazar, E. Zhu, A.K. Amaya, S.H.Y. Liao, S. Scott, E. Sallard, K.L. Dilworth, et al., *Attenuation of Heparan Sulfate Proteoglycan Binding Enhances In Vivo Transduction of Human Primary Hepatocytes with AAV2*. Mol Ther Methods Clin Dev, 2020. **17**: p. 1139-1154.
36. Cao, O., E. Dobrzynski, L. Wang, S. Nayak, B. Mingle, C. Terhorst, and R.W. Herzog, *Induction and role of regulatory CD4+CD25+ T cells in tolerance to the transgene product following hepatic in vivo gene transfer*. Blood, 2007. **110**(4): p. 1132-40.
37. Nydegger, U.E., D.T. Fearon, and K.F. Austen, *The modulation of the alternative pathway of complement in C2-deficient human serum by changes in concentration of the component and control proteins*. J Immunol, 1978. **120**(4): p. 1404-8.

38. Dreismann, A.K., M.E. McClements, A.R. Barnard, E. Orhan, J.P. Hughes, P.J. Lachmann, and R.E. Maclaren, *Functional expression of complement factor I following AAV-mediated gene delivery in the retina of mice and human cells*. *Gene Ther*, 2021.
39. Rose, K.L., D. Paixao-Cavalcante, J. Fish, A.P. Manderson, T.H. Malik, A.E. Bygrave, T. Lin, S.H. Sacks, M.J. Walport, H.T. Cook, et al., *Factor I is required for the development of membranoproliferative glomerulonephritis in factor H-deficient mice*. *J Clin Invest*, 2008. **118**(2): p. 608-18.
40. Cunningham, S.C., A.P. Dane, A. Spinoulas, and I.E. Alexander, *Gene Delivery to the Juvenile Mouse Liver Using AAV2/8 Vectors*. *Molecular Therapy*, 2008. **16**(6): p. 1081-1088.
41. Xiao, X., J. Li, and R.J. Samulski, *Production of high-titer recombinant adeno-associated virus vectors in the absence of helper adenovirus*. *J Virol*, 1998. **72**(3): p. 2224-32.
42. Dane, A.P., S.J. Wowro, S.C. Cunningham, and I.E. Alexander, *Comparison of gene transfer to the murine liver following intraperitoneal and intraportal delivery of hepatotropic AAV pseudo-serotypes*. *Gene Ther*, 2013. **20**(4): p. 460-4.
43. Macanovic, M., D. Sinicropi, S. Shak, S. Baughman, S. Thiru, and P.J. Lachmann, *The treatment of systemic lupus erythematosus (SLE) in NZB/W F1 hybrid mice; studies with recombinant murine DNase and with dexamethasone*. *Clinical & Experimental Immunology*, 1996. **106**(2): p. 243-252.
44. Manderson, A.P., F. Carlucci, P.J. Lachmann, R.A. Lazarus, R.J. Festenstein, H.T. Cook, M.J. Walport, and M. Botto, *The in vivo expression of actin/salt-resistant hyperactive DNase I inhibits the development of anti-ssDNA and anti-histone autoantibodies in a murine model of systemic lupus erythematosus*. *Arthritis Res Ther*, 2006. **8**(3): p. R68.
45. Jablonski, P., B.O. Howden, D.A. Rae, C.S. Birrell, V.C. Marshall, and J. Tange, *An experimental model for assessment of renal recovery from warm ischemia*. *Transplantation*, 1983. **35**(3): p. 198-204.

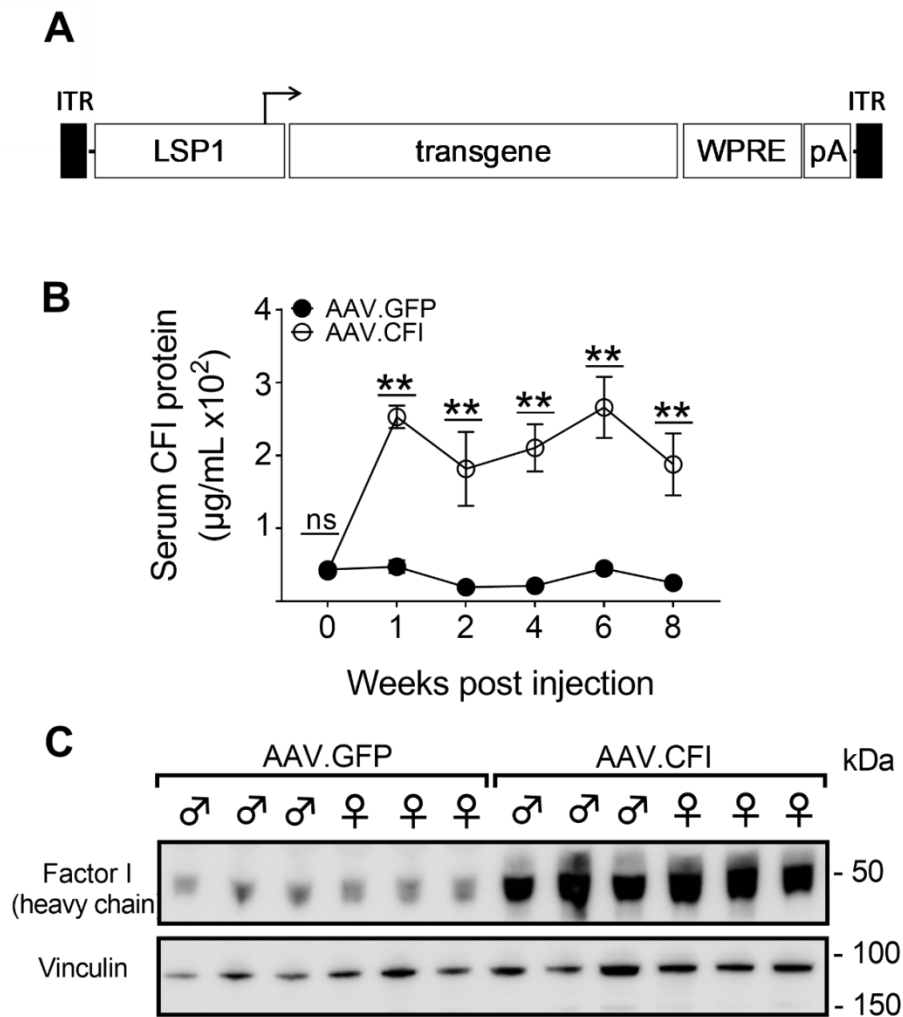


Figure 2: AAV liver transduction induces elevated levels of serum CFI.

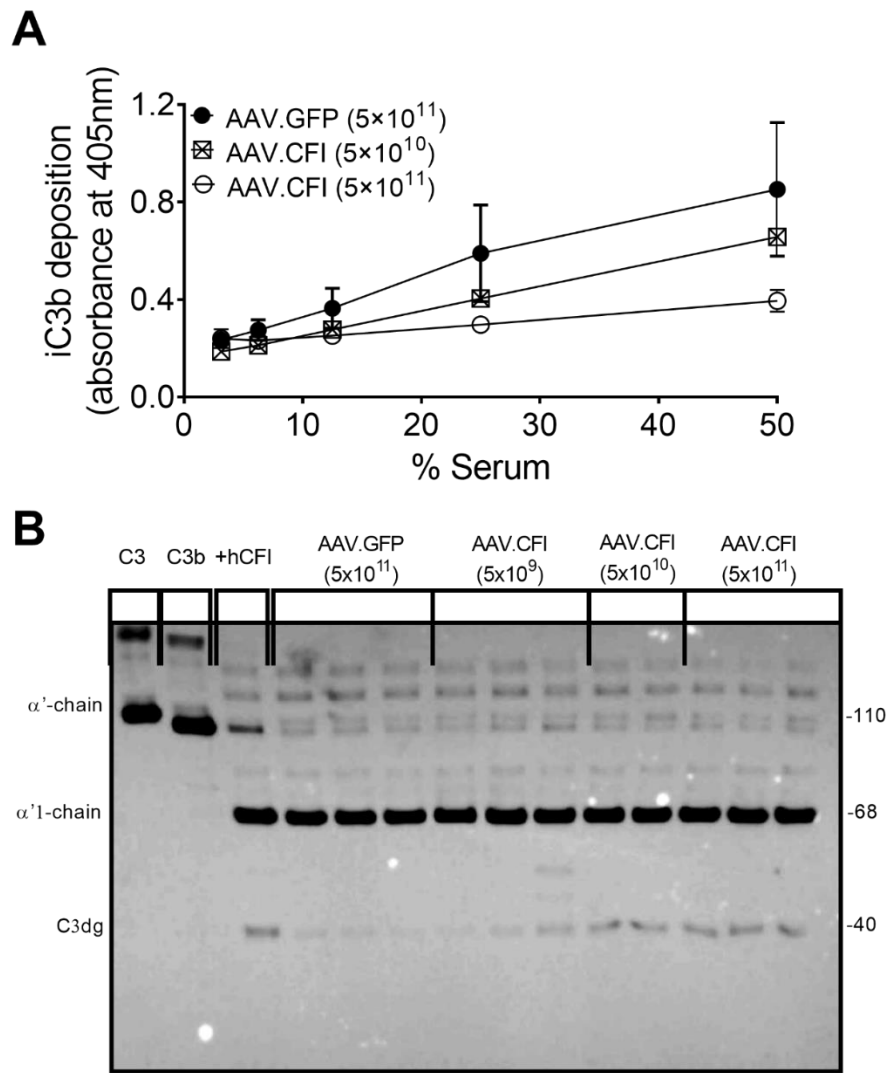


Figure 3: Elevated levels of serum CFI favours the AP degradation cycle.

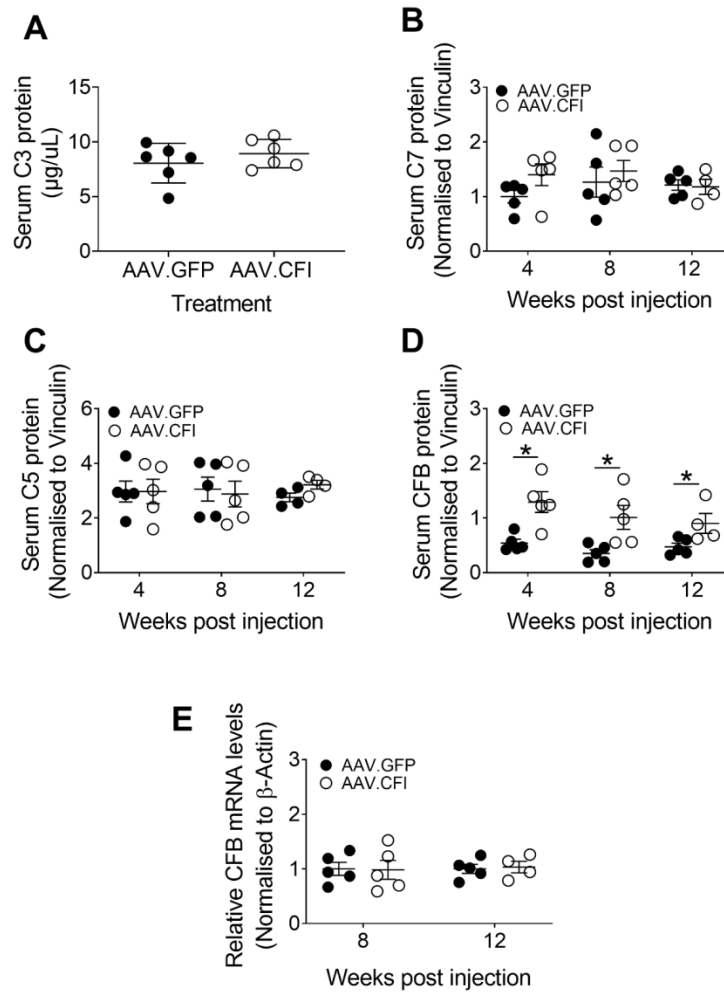


Figure 4: Serum protein and liver transcription analysis of complement proteins after vector treatment.

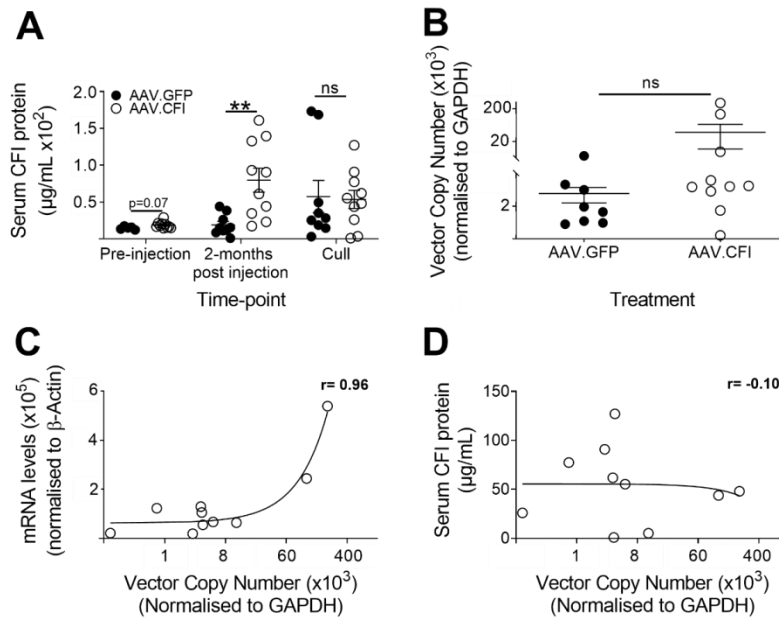


Figure 5: Expression of CFI after AAV.CFI vector transduction in lupus-prone NZBWF1 mice.

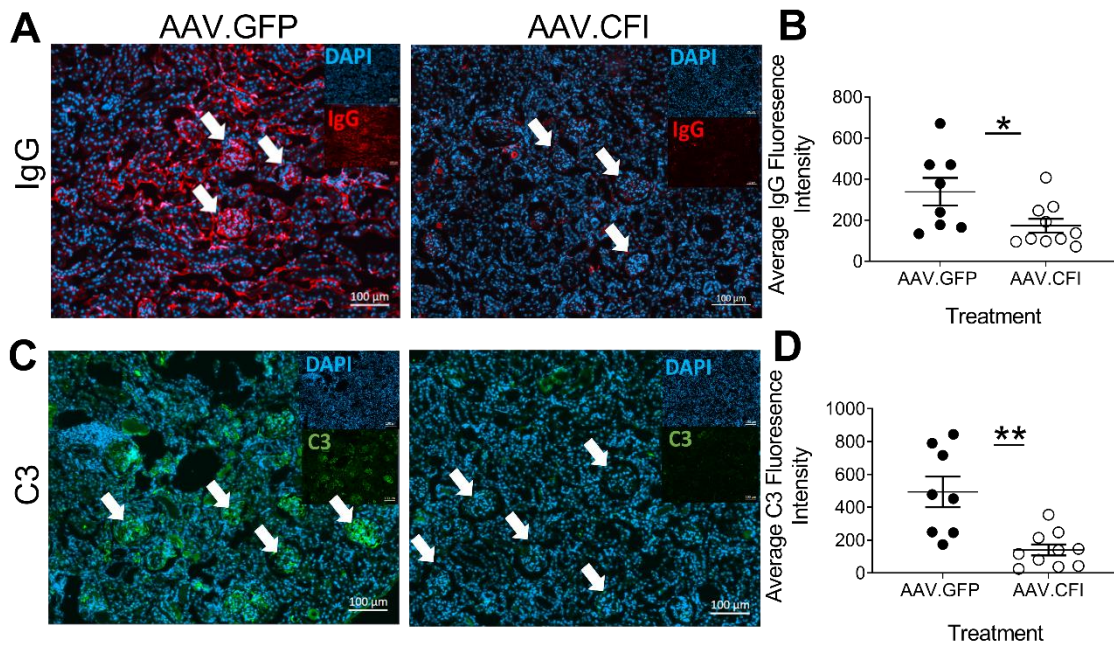


Figure 6: AAV.CFI reduces kidney IgG and C3 deposition in the NZBWF1 mice.

